

## Homology Modeling of the Catalytic Domains of Gelatinases and Docking Study with Their Inhibitors

Yoriko Iwata<sup>a</sup>, Reiko Ohiwa<sup>a</sup>, Kazuhiko Tamaki<sup>b</sup>, Tomoyuki Shibata<sup>a</sup>,  
Aki Matsubara<sup>c</sup>, Kazuhiko Tanzawa<sup>c</sup> and Shuichi Miyamoto<sup>a\*</sup>

<sup>a</sup>Exploratory Chemistry Research Laboratories, <sup>b</sup>Medicinal Chemistry Research Laboratories, and  
<sup>c</sup>Biological Research Laboratories, Sankyo Co., Ltd., 1-2-58,  
Hiromachi, Shinagawa-ku, Tokyo 140-8710, Japan

\*E-mail: miya@shina.sankyo.co.jp

(Received December 15, 2000; accepted January 20, 2001; published online March 30 2001)

### Abstract

Three-dimensional models of the gelatinase catalytic domains were built from collagenase structures by the homology modeling technique. The docking of different types of inhibitors was then studied in an attempt to obtain structural insight into their binding modes. In the case of an amide compound docked with gelatinase A, almost the same binding mode was obtained as that observed in the crystal structure of another amide compound complexed with collagenase. With respect to our series of matlystatin analogs, the key hydrogen bonding and hydrophobic interactions with gelatinase B were similar to those of the above amide compounds, although these derivatives have a unique piperazine ring. The length and hydrophobic nature of the S1' subsite was well consistent with the observation that the inhibitory activity rises as the alkyl chain at P1' becomes longer. The binding mode of a sulfonamide inhibitor was slightly different from that of amide and piperazine inhibitors, but similar to that proposed recently for another sulfonamide inhibitor.

**Key Words:** Homology Modeling, Docking Study, MMP, Gelatinase, Collagenase, Inhibitor

**Area of interest:** Molecular Recognition

### Introduction

The matrix metalloproteinases (MMPs) are a family of zinc-dependent proteinases that degrade different macromolecular components of the extracellular matrix and basement membranes. These

enzymes have been implicated in matrix remodeling events of connective tissues during embryonic growth and wound healing [1, 2]. The members of this family can be classified into several different groups on the basis of their substrate specificities: collagenases (MMP-1, -8, -13), gelatinases (MMP-2, -9), stromelysins (MMP-3, -10, -11), membrane-type MMPs (MMP-14, -15, -16, -17), and others (e.g. MMP-7).

MMPs share several features: a highly similar N-terminal catalytic domain, requirement for a zinc ion at the active site, and their secretion as inactive proenzymes [3]. In the case of gelatinases, the structurally independent fibronectin-like domain is inserted into the catalytic domain. The three-dimensional (3D) structures of catalytic domains of a number of MMPs including MMP-1, -3, and -8 have been recently determined by X-ray crystallography and NMR spectroscopy [4–7], although those of the gelatinases have not.

At elevated levels, gelatinases expressed by certain tumor cells cleave the vascular basement membrane, which consists of type IV collagen, and this may lead to metastasis [8, 9]. Gelatinases have also been involved in the process of angiogenesis [10, 11], which is essential for the growth of solid tumours. Thus, gelatinase inhibitors have been researched as a new type of anticancer drug [12, 13].

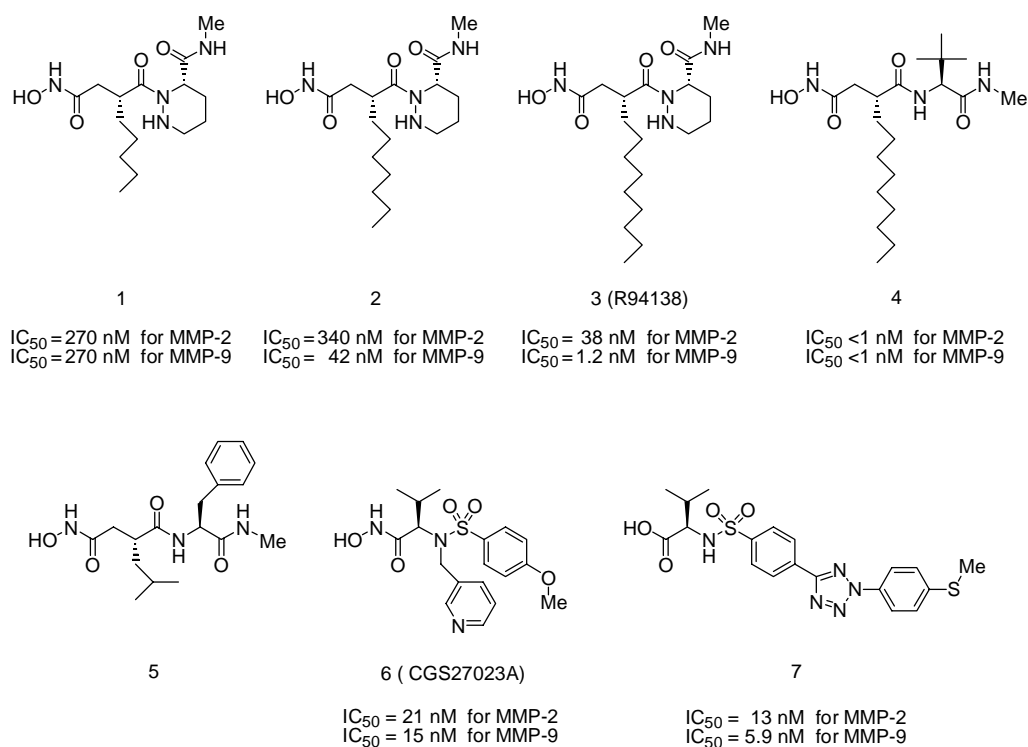


Figure 1. Chemical structures and inhibitory activities (IC<sub>50</sub>) against MMP-2 and MMP-9. IC<sub>50</sub> was determined with <sup>3</sup>H-acetyl gelatin, for substrate, as reported in [14] with slight modifications. By this procedure, compound **4** appeared to be very potent. Alternatively, a fluorescent assay was carried out by incubating 100  $\mu$ L of assay mixture with 20  $\mu$ M Knight's substrate (Mca-Pro-Leu-Gly-Leu-Dps-Ala-Arg-NH<sub>2</sub>) [15], enzyme solution in 50 mM Tris-HCl (pH 7.5), 0.2 M NaCl, 10 mM CaCl<sub>2</sub>, and 0.05% Brij35, at 37°C for 30 min. The time-course of fluorescence was measured at  $\lambda_{ex}$ =355 nm and  $\lambda_{em}$ =405 nm with an ARVO SX 1420 Multilabel Counter (Wallac) and the initial velocity was also estimated. In this fluorescent assay, the IC<sub>50</sub> values against MMP-9 were 0.12 and 9.8 nM for compounds **4** and **6**, respectively. The IC<sub>50</sub> value of **7** was taken from [16].

Many compounds are known to inhibit gelatinases, and most of them contain a carboxylic acid or hydroxyamic acid moiety [13]. We have found that a series of matlystatin analogs (**1–3**) with a unique piperazine skeleton have potent inhibitory activities against gelatinases and that the potency rises as the alkyl side chain becomes longer (Figure 1) [14]. Recently, sulfonamide compounds were also reported to exert good inhibition [16, 17]. Although the carboxylic acid or hydroxyamic acid group of inhibitors is thought to coordinate the zinc ion in the active site, their detailed binding modes are not well established as there were no crystal structures of these enzymes. We, therefore, decided to construct 3D models of gelatinases from the crystal structures of other MMPs by using the homology modeling technique and to perform the docking study for different types of inhibitors in an attempt to obtain structural insight into their binding modes.

	107	126
MMP-2 : (Gelatinase-A)	PKWDKNQITYRIIGYTPDL	
MMP-9 : (Gelatinase-B)	LKWHHHNITYWIQNYSEDLP	
MMP-1 : (fibroblast collagenase)	PRWEQTHLTYRIENYTPDL	
MMP-8 : (neutrophil collagenase)	PKWERTNLTYRIRNYTPQLS	
MMP-3 : (stromelysin)	PKWRKTHLTYRIVNYTPDL	
	==β1==	
	127	178
MMP-2 : PETVDDAFARAFQVMSDVTPLRFSRIHDGEADIMINFGRWEHGDGYPFDGKD		
MMP-9 : RAVIDDAFARAFALWSAVTPLTFTRVYSRDADIVIQFGVAEHGDGYPFDGKD		
MMP-1 : RADVDHAIEKAFQLWSNVTPLTFTKVSEGGADIMISFVRGDHRDNSPFDGPG		
MMP-8 : EAEVERAIKDAFELWSVASPLIFTRISQGEADINIAFYQRDHGDNPSFDPGN		
MMP-3 : KDAVDSAVEKALKVWEEVTPLTFSRLYEAGEADIMISFAVREHGDYFPFDGPG		
	===== α1 ===== == β2== == β3==	
	179	207
MMP-2 : GLLAHAFAPGTGVGGDSHFDDDELWTLGE-#-QGYSLF	LV	AAHEFGHAMG
MMP-9 : GLLAHAFPPGPGIQQDAHFDDDELWSLGD-#-QGYSLF	LV	AAHEFGHALG
MMP-1 : GNLAHAFQPGPGIGGDAHFDEDERWTNNF---REYNLH	RV	AAHELGHSLG
MMP-8 : GILAHAFQPGQGIGGDAHFDAEETWTNTS---ANYNLF	LV	AAHEFGHSLG
MMP-3 : NVLAHAYAPGPGINGDAHFDDDEQWTKDT---TGTNLF	LV	AAHEIGHSLG
	=β4= ==β5== ===== α2 =====	
	226	261
MMP-2 : LEHSQDP	GALMA PIYT Y...TKNFRLS	QDDIKGIQELYG
MMP-9 : LDHSSVP	EALMY PMYR F...TEGPPLH	KDDVNGIRHLYG
MMP-1 : LSHSTDI	GALMY PSYT F...SGDVQLA	QDDIDGIQAIYG
MMP-8 : LAHSSDP	GALMY PNYA FR.ETSNYSLP	QDDIDGIQAIYG
MMP-3 : LFHSANT	EALMY PLYH SLTDLTRFRLS	QDDINGIQSLYG
	==== α3 ===	

Figure 2. Sequence alignment of a representative set of the catalytic domains of MMPs. The secondary structure elements ( $\alpha$ -helix:  $\alpha 1$ – $\alpha 3$ ;  $\beta$ -strand:  $\beta 1$ – $\beta 5$ ) and the residue numbering were taken from the X-ray structure of MMP-1 (1CGE). Gaps are denoted by dots, and the fibronectin-like domain is indicated by #. The residues forming the S1' subsite are enclosed by rectangles.

Homology modeling is widely used to build protein models based on the known 3D structures of proteins that have sequence similarity to that of the target protein [18–20]. Generally, homology

modeling with a sequence identity of >50% is expected to give a model accurate enough to be used for the subsequent modeling work and analysis of protein–ligand interactions. Figure 2 shows the sequence alignment of the catalytic domains of gelatinases (MMP-2, -9) with those of known 3D structures, MMP-1 (fibroblast collagenase), MMP-8 (neutrophil collagenase), and MMP-3 (stromelysin-1). The S1' subsite is not well conserved among MMPs and is generally considered as the substrate specificity site of MMPs. We selected MMP-1 as the reference protein, because it does not have any insertions at the S1' subsite, to which substructures of the inhibitors shown in Figure 1 were considered to bind.

Although several X-ray crystallographic studies of MMPs have been reported, none of the atomic coordinates were available at the start of this project. We, therefore, reconstructed a 3D model of MMP-1 from a pair of stereographic figures found in the literature [4]. An MMP-2 (gelatinase A) model was then built from the MMP-1 model by the homology modeling technique, and the complex structure with amide compound **4**, a highly potent inhibitor, was obtained. In the meantime, a crystal structure of MMP-1 [5] was released in the Protein Data Bank (PDB) [21]. Based on the atomic coordinates of MMP-1, an MMP-9 (gelatinase B) model complexed with **4** was built. With this model, a docking study was carried out with our piperazine inhibitors as well as a known sulfonamide inhibitor, **6** (CGS27023A) (Figure 1). Finally, our results were compared with those obtained by the homology modeling of gelatinases and docking simulations of sulfonamide inhibitors, which was recently reported by Yodo et al. [22].

## Results and Discussion

### Reconstruction of the 3D model of collagenase

First, the 3D coordinates of the  $\alpha$ -carbon atoms of MMP-1 were reconstructed from a pair of stereographic figures taken from the literature by using the ReconstC $\alpha$  program [23]. Next, the backbone structure was rebuilt with the in-house program. The side chains were then added and optimized using the rotamer library [24]. Finally, compound **5** was docked with the model as was illustrated in the literature [4], and the complex structure was geometry optimized with molecular mechanics and dynamics calculations to produce the final model of MMP-1.

Since the atomic coordinates of the enzyme are now available in the PDB under the code name of 1HFC, the deviation of the reconstructed model from the correct crystal structure was examined. The root mean square (rms) deviation of the C $\alpha$  atom was 1.4 Å for the starting C $\alpha$  model as well as for the final complete model. The deviation was rather large compared with those reported for the test cases [23]. There are two reasons for this. First is that the resolution was not high enough because the figures were printed in color with thick lines. Second is that the enzyme structure was overlapped with that of thermolysin, making some parts more difficult to read.

The rms deviation of the backbone atoms in the final model from the canonical coordinates was 1.5 Å. It seemed that more than half of the deviations were due to the slight deformation of the whole protein 3D structure. In fact, local orientations of the backbone peptide planes were well reproduced. The number of residues whose main chain torsional angles ( $\phi$ ,  $\psi$ ) were located in the disallowed region of the Ramachandran plot was only six. The side chain torsional angle  $\chi_1$  is reasonably constructed with the rms deviation of  $\sim 50^\circ$ . The side chain conformations of the ligand binding site were well built since they were modeled in reference to the magnified figure of the site as found in the literature.

## Homology modeling of gelatinase A

From the sequence alignment shown in Figure 2 we have substituted the side chains of MMP-1 with those of MMP-2 and optimized their conformations by using the rotamer library. The resulting model was complexed with the amide compound **4** and energy minimized to produce the final complex model of MMP-2.

As it can be easily imagined from the high sequence homology, the constructed 3D structure of MMP-2 was rather similar to that of MMP-1. In particular, the shape of the catalytic site and the S'-subsite groove, which is considered to be involved in the binding of the substrate backbone, was essentially the same for both of the two models. The binding mode of amide compound **4** corresponded well with that of **5** complexed with MMP-1. Figure 3 shows the ligand binding site of the complex model of MMP-2. The walls of the narrow groove of the S' subsites consist of Gly179–Ala182 and Pro238–Tyr240. The *tert*-butyl group of **4** is situated between the hydrophobic side chains of Pro238, Met239, and Leu180.

A distinct difference between the MMP-1 and -2 models was found in the S1' subsite. The subsite of the MMP-2 model was channel-like, whereas that of MMP-1 was pocket-like. The main reason for the enlargement of the subsite in MMP-2 was considered to be the decrease of the side chain size due to a mutation from Arg214 in MMP-1 into Leu214 in MMP-2 (Figure 2). In fact, Stams et al. reported that the replacement of Arg214 in the MMP-1 by Leu in MMP-8 (neutrophil collagenase) substantially enlarges the S1' pocket [7]. The length of the S1' channel corresponded approximately to the methylene chains of 9–10 carbon atoms at the P1' position as can be seen in Figure 3.

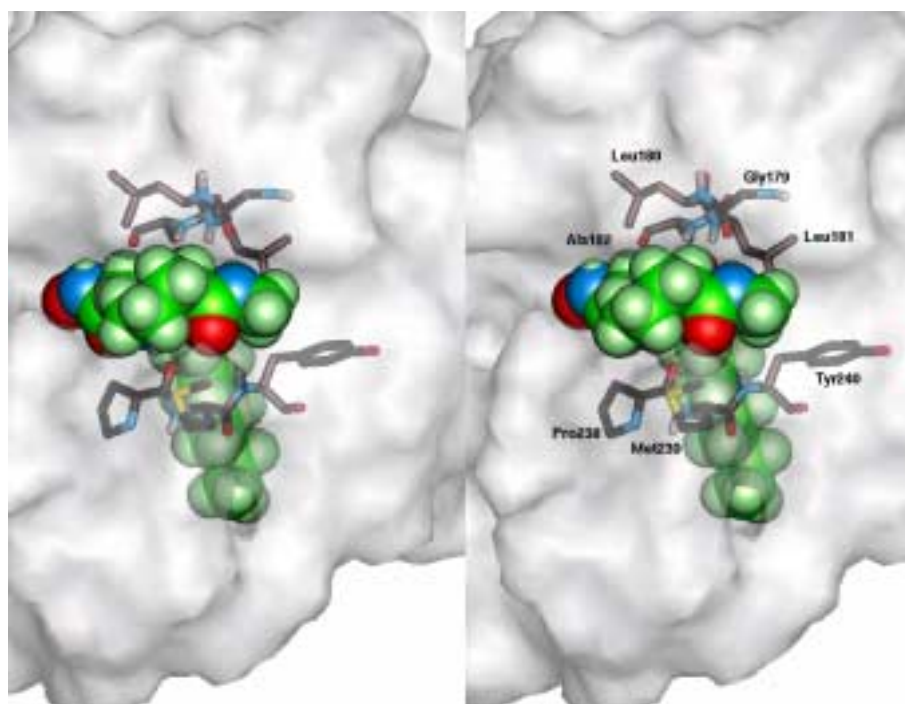
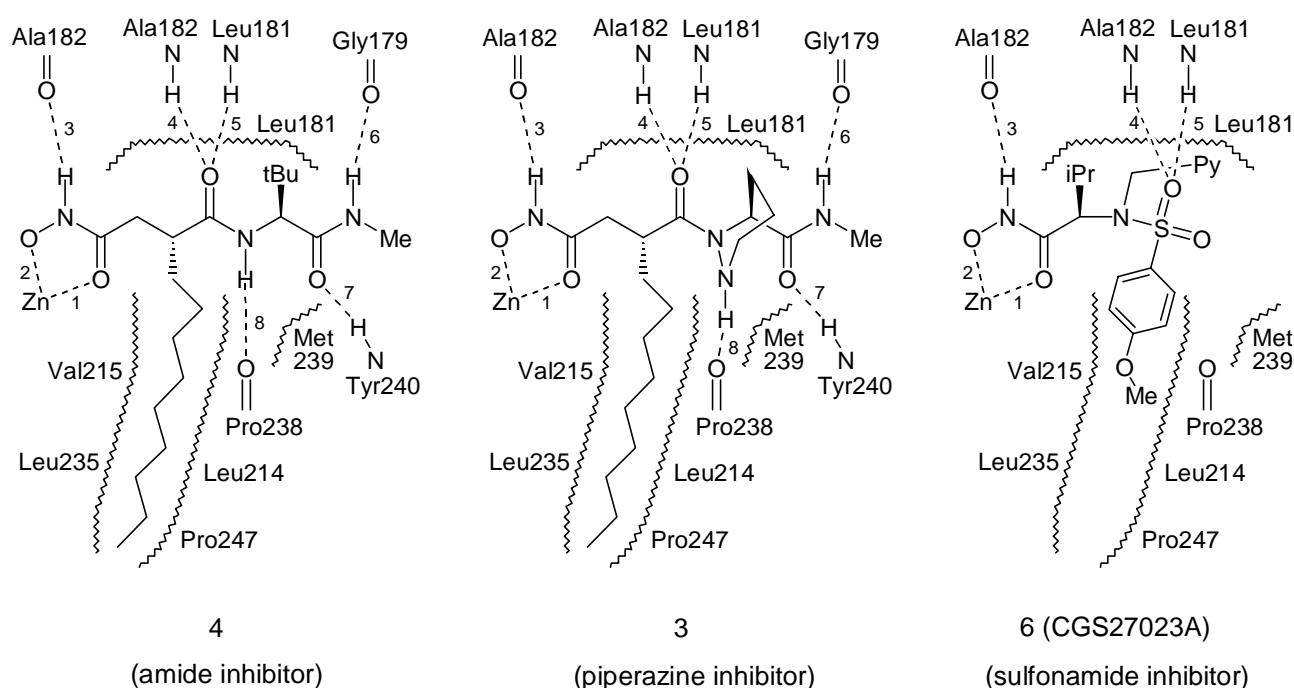


Figure 3. Complex structure model of the gelatinase B binding site and **4**. Connolly surface of the enzyme is translucently shown in gray. Selected residues of gelatinase B (black) and **4** (green) are represented in stick and CPK forms, respectively, in which oxygen is shown in red, nitrogen in blue, and sulfur in yellow. Most of the hydrogen atoms of gelatinase B are omitted for clarity.

## Homology modeling of gelatinase B

Similarly to the modeling of gelatinase A, the complex model of gelatinase B with amide compound **4** was constructed from the crystal structure of MMP-1 (1CGE) [5]. The rms deviation of the backbone atoms of the two reference crystal structures of MMP-1 (1HFC and 1CGE) was only 0.37 Å. The 3D structure of MMP-9 was, therefore, rather similar to that of MMP-2. Nevertheless, the size of the S1' subsite of MMP-9 was smaller than that of MMP-2, due to the salt bridge between Glu233 and Arg214 at the bottom of the subsite of MMP-9. The mode of ligand binding to MMP-9 was, however, rather similar to that of MMP-2. The key interactions between the enzyme and **4** are schematically illustrated in Figure 4. Judging from the interatomic distances, the three hydrogen bonds with Leu181, Pro238, and Tyr240 were tight while those involving Ala182 and Gly179 were loose. The alkyl chain at P1' was fitted into the essentially hydrophobic S1' subsite comprised of residues such as Leu214, Val215, Leu235, and Pro247.



Interatomic distance (Å)			
1	2.2	2.1	2.2
2	2.2	2.2	2.1
3	2.7	2.9	2.9
4	2.8	3.0	2.0
5	2.0	2.0	2.5
6	2.5	2.1	—
7	2.0	3.5	—
8	2.1	2.0	—

Figure 4. Schematic drawings of the key interactions between the gelatinase B model and three kinds of inhibitors. Wavy lines represent hydrophobic interactions. Polar interactions are indicated by dotted lines, and the interatomic distances are also given.

## Docking study with gelatinase B

The piperazine and sulfonamide inhibitors (**1–3** and **6**) were docked into the gelatinase B model obtained above. In the case of the piperazine inhibitors, the number of bonds between the hydroxyamic acid group and the NH of the piperazine ring is greater than that of amide inhibitors such as **4** or **5**. Nonetheless the NH group of compounds **1–3** formed hydrogen bond to the same carbonyl group of Pro238 as was observed for **5** bound to MMP-1. Figure 5 shows the binding site of **3**, and its binding mode is schematically drawn in Figure 4. Like the *tert*-butyl group of **4**, the methylene groups in the piperazine ring were involved in the hydrophobic interactions with the side chains mentioned above. Other key interactions between the enzyme and the inhibitor were also similar to those observed for **4** although the magnitudes of the terminal amide moiety interactions with Tyr240 and Gly179 were reversed (Figure 4).

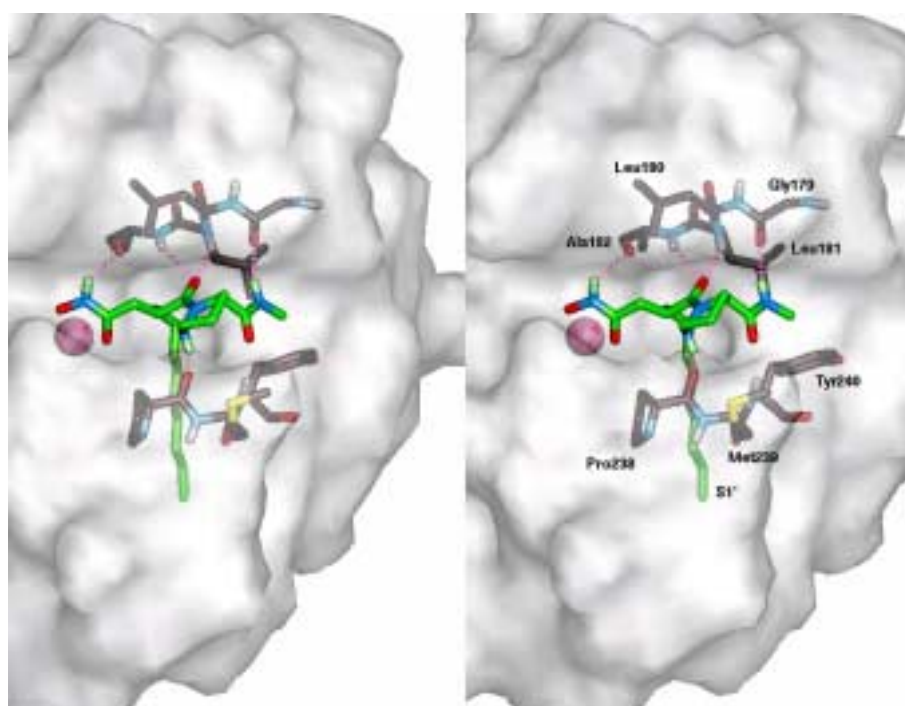


Figure 5. Complex structure model of the gelatinase B binding site and **3**. Connolly surface of the enzyme is translucently shown in gray. Inhibitor **3** (green) and selected residues of gelatinase B (black) are represented in stick forms, in which oxygen is shown in red, nitrogen in blue, and sulfur in yellow. Dashed lines represent polar interactions, and a zinc ion is shown as a pink sphere. Most of the hydrogen atoms are omitted for clarity.

We have already reported that the inhibitory activity against MMP-9 rises as the alkyl chain at the P1' position becomes longer from pentyl to heptyl and then to nonyl in the piperazine derivatives. The length and hydrophobic nature of the S1' subsite was consistent with this observation. In fact, as the buried hydrophobic surface region at the interface between the alkyl chain and the subsite increases from 217 to 300 and then to 393 Å<sup>2</sup> for compounds **1–3**, respectively, the inhibitory potency rises as well.

With respect to **6**, two kinds of docking modes were taken into account: one with the methoxyphenyl group in the S1' pocket of MMP-9 and the other with the pyridine ring there. They

were examined and compared in terms of their favorable states as recognized by the overall interaction energies, and the former was found to be more favored. In this binding mode, one of the sulfonyl oxygen atoms had hydrogen-bonding interactions with the NH group of both Leu181 and Ala182 as schematically shown in Figure 4. Unlike the amide and piperazine compounds, no hydrogen bond to Pro238 was observed in the case of **6** due to the absence of the NH functional group in the P' site. The pyridine moiety was between the hydrophobic walls, which included Leu180, Pro238, and Met239.

Recently, the homology modeling of gelatinase and docking simulations of sulfonamide inhibitors was reported by Yodo et al. [22]. The reference protein they used was stromelysin-1 (MMP-3, PDB code name 1SLM [25]). Although its sequence identity with gelatinases (~58%) is slightly higher than that of MMP-1 (~56%), MMP-3 has three extra residues inserted at the S1' subsite. In fact, it was reported that some difficulties were experienced in constructing the S1' loop. According to the modeling by Yodo et al., MMP-9 has a pocket-like S1' subsite and MMP-2 has a channel-like S1' subsite. In each of our gelatinase models, the S1' subsite was channel-like but the subsite size of MMP-9 was smaller than that of MMP-2. We considered that our obtained models were not inconsistent with those of Yodo et al.

The sulfonamide inhibitors such as **7** reported by Yodo et al. had a carboxylic acid group, which coordinated the zinc ion. In their docking models, the sulfonyl substituent was in the S1' pocket and one of the sulfonyl oxygens also formed hydrogen bonds with the backbone NH of both Leu181 and Ala182. This suggests that the binding mode of the two kinds of sulfonamide inhibitors was essentially the same.

In this modeling study we have elucidated the similarities and differences among the binding modes of different types of gelatinase inhibitors. This may be useful for interpreting structure-activity relationships of known inhibitors as well as designing new inhibitors.

## Conclusion

We have constructed 3D models of gelatinases from fibroblast collagenase structures by the homology modeling technique. With the constructed model, the docking study was performed with different types of inhibitors. In the case of amide inhibitor **4** complexed with MMP-2, almost the same binding mode as that observed in the crystal structure of amide compound **5** complexed with MMP-1 was obtained. With respect to the piperazine compounds, the key hydrogen bonding and hydrophobic interactions with MMP-9 were similar to those of amide compound **4**. The length and hydrophobic nature of the S1' subsite was well consistent with the observation that the inhibitory activity rises as the alkyl chain at P1' becomes longer from pentyl to heptyl and then to nonyl groups. The binding mode of sulfonamide inhibitor **6** was essentially the same as that presented by Yodo et al. for **7**.

## Computational Procedure

### Software and hardware

The QUANTA/CHARMm system [26] was used throughout the modeling study except when mentioned otherwise. The PROTEIN module of the QUANTA system was used for the homology modeling. The Adopted-Basis Newton Raphson algorithm was used to perform the energy minimization [27]. Calculations were mainly run on Silicon Graphics INDIGO2 or O2

workstations.

### Reconstruction of the 3D model of collagenase

The ReconstC $\alpha$  program was used to reconstruct the 3D coordinates of  $\alpha$ -carbon atoms from a pair of stereographic figures of a C $\alpha$  trace [23]. The stereographic figures presented by Spurlino et al. [4] were used because they were the only ones for MMP-1 (1HFC) when this study started. The backbone structure was rebuilt with the in-house program. After adding the appropriate side chains, the conformations were optimized by using the Ponder and Richards's rotamer library [24] equipped with the PROTEIN module of the QUANTA system. With respect to the ligand binding site, the side chain conformations were modeled in reference to the magnified figure of the site with the side chain structures as shown in the literature [4].

After compound **5** was docked with the MMP-1 model as shown in the literature, the complex structure was initially energy minimized with a harmonic distance constraint of 25 kcal/mol $\cdot\text{\AA}^2$  between the enzyme and metal ions as well as the ligand. The constraint distances were based on those reported for the coordinations with the metal ions and for the hydrogen bonds to the ligand [4]. The complex structure was then subjected to the molecular dynamics calculation for 40 ps at 400 K. During this simulated annealing, the distance constraint as well as the positional constraints of 25 and 5 kcal/mol $\cdot\text{\AA}^2$  for C $\alpha$  and other backbone atoms, respectively, were applied. After cooling the system, the resulting structure was energy minimized to produce the final complex model of MMP-1.

### Homology modeling of gelatinases

Amino acid sequences of MMPs used in this study were taken from the work done by Henderson et al. [28] except for MMP-8, whose sequence was taken from the work done by Bode et al. [29]. A multiple sequence alignment was performed with respect to the catalytic domain residues without the fibronectin-like domain. The alignment was then slightly modified taking the 3D structural information of the crystal structures into account.

From the sequence alignment described above, we have mutated the side chains of MMP-1 into those of MMP-2 and -9. The conformations of the mutated residues were optimized with the Ponder and Richards's rotamer library. Those side chains common between gelatinases and fibroblast collagenase were held fixed during the optimization. This was based on studies in which it was elucidated that topologically equivalent side chains in homologous structures generally adopt the same conformations [30].

After compound **4** with high potency was docked into the gelatinase model, the ligand structure was initially energy minimized with the same distance constraints as those applied for MMP-1 with the protein structure fixed. The whole complex structure was then energy minimized with the harmonic distance constraint as well as the positional constraints of 25 and 5 kcal/mol $\cdot\text{\AA}^2$  for C $\alpha$  and other backbone atoms, respectively. The resulting complex structure was subjected to molecular dynamics calculations for 40 ps at 400 K. During this simulated annealing, the distance constraint as well as the weak positional constraints of 5 and 1 kcal/mol $\cdot\text{\AA}^2$  for C $\alpha$  and other backbone atoms, respectively, were applied. After cooling the system, the structure was energy minimized without any constraints to produce the final complex model of gelatinase.

## Docking study with gelatinase B

The piperazine and sulfonamide inhibitors were initially fitted into the binding site of the gelatinase B model similarly to amide compound **4**. The ligand structure was energy minimized with the protein structure fixed. In the case of the piperazine inhibitors, a conformational search of the alkyl chain docked in the S1' subsite was performed. First, the stable complex structures of **1** were searched by changing the side chain torsional angles in 120° increments. The ligand conformation of the most stable complex model of **1** was then used in the conformational search of **2** which has longer side chain. The ligand conformation of the most stable complex model of **2** was then employed in the conformational search of **3**, which has the longest side chain among the three inhibitors. With respect to the sulfonamide inhibitor, two kinds of docking modes were considered: one with the methoxyphenyl group in the S1' pocket and the other with the pyridine ring there. The conformations of the methoxyphenyl and pyridine groups were manually examined to afford stable complex structures. The most stable complex structure of each inhibitor was finally geometry-optimized with the protein side chains within 8 Å from the ligand allowed to relax. The buried hydrophobic surface areas at the protein–ligand interface were calculated with respect to the alkyl chains of compounds **1–3**.

## References

- [1] G. J. Murphy, G. Murphy and J. J. Reynolds, *FEBS Lett.*, **289**, 4-7 (1991).
- [2] A. M. Pendás, V. Knäuper, X. S. Puente, E. Liano, M.-G. Mattei, S. Apte, G. Murphy and C. López-Otín, *J. Biol. Chem.*, **272**, 4281-4286 (1997).
- [3] D. Muller, B. Quantin, M.-C. Gesnel, R. Millon-Collard, J. Abecassis and R. Breathnach, *Biochem. J.*, **253**, 187-192 (1988).
- [4] J. C. Spurlino, A. M. Smallwood, D. D. Carlton, T. M. Banks, K. J. Vavra, J. S. Johnson, E. R. Cook, J. Falvo, R. C. Wahl, T. A. Pulvino, J. J. Wendoloski and D. L. Smith, *Proteins: Struct. Funct. Genet.*, **19**, 98-109 (1994).
- [5] B. Lovejoy, A. M. Hassell, M. A. Luther, D. Weigel and S. R. Jordan, *Biochemistry*, **33**, 8207-8217 (1994).
- [6] P. R. Gooley, J. F. O'Connell, A. I. Marcy, G. C. Cuca, S. P. Salowe, B. L. Bush, J. D. Hermes, C. K. Esser, W. K. Hagmann, J. P. Springer and B. C. Johnson, *Nat. Struct. Biol.*, **1**, 111-118 (1994).
- [7] T. Stams, J. C. Spurlino, D. L. Smith, R. C. Wahl, T. F. Ho, M. W. Qoronfleh, T. M. Banks and B. Rubin, *Nat. Struct. Biol.*, **1**, 119-123 (1994).
- [8] N. R. A. Beeley, P. R. J. Ansell and A. J. P. Docheerty, *Curr. Opin. Thera. Patents*, **4**, 7-16 (1994).
- [9] A. H. Davidson, A. H. Drummond, W. A. Galloway and M. Whittaker, *Chem. Ind.*, **1997**, 258-261.
- [10] R. E. Galaray, D. Grobelny, H. G. Foellmer and L. A. Fernandez, *Cancer Res.*, **54**, 4715-4718 (1994).
- [11] G. Bergers, R. Brekken, G. McMahon, T. H. Vu, T. Itoh, K. Tamaki, K. Tanzawa, P. Thorpe, S. Itohara, Z. Werb and D. Hanahan, *Nat. Cell Biol.*, **2**, 737-744 (2000).
- [12] J. R. Porter, T. A. Millican and J. R. Morphy, *Curr. Opin. Thera. Patents*, **5**, 1287-1295 (1995).
- [13] R. P. Beckett, A. H. Davidson, A. H. Drummond, P. Huxley and M. Whittaker, *Drug Discov. Today*, **1**, 16-26 (1996).

- [14] K. Tamaki, K. Tanzawa, S. Kurihara, T. Oikawa, S. Monma, K. Shimada and Y. Sugimura, *Chem. Pharm. Bull.*, **43**, 1883-1893 (1995).
- [15] C. G. Knight, F. Willenbrock and G. Murphy, *FEBS Lett.*, **296**, 263-266 (1992).
- [16] Y. Tamura, F. Watanabe, T. Nakatani, K. Yasui, M. Fuji, T. Komurasaki, H. Tsuzuki, R. Maekawa, T. Yoshioka, K. Kawada, K. Sugita and M. Ohtani, *J. Med. Chem.*, **41**, 640-649 (1998).
- [17] J. R. Morphy, T. A. Millican and J. R. Porter, *Curr. Med. Chem.*, **2**, 743-62 (1995).
- [18] T. L. Blundell, B. L. Sibanda, M. J. E. Sternberg and J. M. Thornton, *Nature*, **326**, 347-352 (1987).
- [19] J. Singh, E. M. Dobrusin, D. W. Fry, T. Haske, A. Whitty and D. J. McNamara, *J. Med. Chem.*, **40**, 1130-1135 (1997).
- [20] A. Marsh and D. M. Ferguson, *Proteins: Struct. Funct. Genet.*, **28**, 217-226 (1997).
- [21] H. M. Berman, J. Westbrook, Z. Feng, G. Gilliland, T. N. Bhat, H. Weissig, I. N. Shindyalov and P. E. Bourne, *Nucleic Acids Res.*, **28**, 235-242 (2000).
- [22] R. Kiyama, Y. Tamura, F. Watanabe, H. Tsuzuki, M. Ohtani and M. Yodo, *J. Med. Chem.*, **42**, 1723-38 (1999).
- [23] Y. Iwata, A. Kasuya and S. Miyamoto, *J. Comput.-Aided Mol. Design*, **10**, 558-566 (1996).
- [24] J. W. Ponder and F. M. Richards, *J. Mol. Biol.*, **193**, 775-791 (1987).
- [25] J. W. Becker, A. I. Marcy, L. L. Rokosz, M. G. Axel, J. J. Burbaum, P. M. Fitzgerald, P. M. Cameron, C. K. Esser, W. K. Hagmann, J. D. Hermes and J. P. Springer, *Protein Sci.*, **4**, 1966-1976 (1995).
- [26] Molecular Simulations, Inc: San Diego, California, USA; URL = <http://www.msi.com>.
- [27] B. R. Brooks, R. E. Bruccoleri, B. D. Olafson, D. J. States, S. Swaminathan and M. Karplus, *J. Comput. Chem.*, **4**, 187-217 (1983).
- [28] B. Henderson, A. J. P. Docherty and N. R. A. Beeley, *Drugs Future*, **15**, 495-508 (1990).
- [29] W. Bode, P. Reinemer, R. Huber, T. Kleine, S. Schnierer and H. Tschesche, *EMBO. J.*, **13**, 1263-1269 (1994).
- [30] N. L. Summers, W. D. Carlson and M. Karplus, *J. Mol. Biol.*, **196**, 175-198 (1987).

## ゼラチナーゼ活性ドメインのホモロジーモデリングと阻害剤とのドッキングスタディ

岩田依子<sup>a</sup>、大岩玲子<sup>a</sup>、玉木和彦<sup>b</sup>、柴田智之<sup>a</sup>、松原亜紀<sup>c</sup>、丹沢和比古<sup>c</sup>、  
宮本秀一<sup>a\*</sup>

三共株式会社、<sup>a</sup>創薬化学研究所、<sup>b</sup>化学研究所、<sup>c</sup>第二生物研究所

\*E-mail: miya@shina.sankyo.co.jp

### 要旨

ホモロジーモデリング手法によりコラーゲナーゼの構造からゼラチナーゼの立体構造モデルを構築した。そのモデルを利用していくつかのタイプの異なる阻害剤とのドッキングスタディを実施し、それぞれの相互作用様式を考察した。アミド型阻害剤のゼラチナーゼAとのドッキングでは、コラーゲナーゼ複合体結晶構造中の他のアミド型阻害剤と同様の結合様式が得られた。マトリスタチン類縁体はユニークなピペラジン環を有するにもかかわらず、ゼラチナーゼBとの主要な水素結合ならびに疎水性相互作用はアミド型と同様であった。また、S1'サブサイトが細長く疎水性であることは、P1'のアルキル鎖が長くなるにしたがって阻害活性が上昇することと一致するものであった。スルホンアミド型阻害剤の結合様式は、アミド型やピペラジン型阻害剤と若干異なるものの、最近報告された他のスルホンアミド型阻害剤の複合体モデルにおける結合様式と同様であった。

**キーワード：**ホモロジーモデリング、ドッキングスタディ、MMP、ゼラチナーゼ、コラーゲナーゼ、阻害剤

**領域区分：**分子認識